Japanese Journal of Applied Physics
Vol. 47, No. 8, 2008, pp. 6757–6759

III–Nitride-Based Microarray Light-Emitting Diodes with Enhanced Light Extraction Efficiency

Mount-Learn WU*, Yun-Chih LEE, Po-Shen LEE, Cheng-Huang KUO, and Jenq-Yang CHANG

Department of Optics and Photonics, National Central University, Jhongli, Taiwan 32001, R.O.C.

(Received January 15, 2008; revised March 26, 2008; accepted April 30, 2008; published online August 22, 2008)

In this paper, the enhancement of light extraction efficiency in III–nitride-based light-emitting diodes (LEDs) with an array of microstructures is demonstrated numerically and experimentally at the near-ultraviolet (n-UV) spectral region. Two different microstructures are adopted to study the mechanism, including the shallow etching of microstructures on the indium–tin-oxide (ITO) p-contact and the deep etching of microholes through the InGaN/GaN multiple-quantum-well (MQW) active structure and down to the n-type GaN layer. Multiple point sources with TE and TM polarizations in the MQW region are utilized in the finite-difference time domain (FDTD) analysis to model the behaviour of LED. The simulated beam patterns of both LEDs reveal that the microstructures act as diffraction gratings to extract guided light in the n-type GaN layer. The measured results of beam patterns also verify the prediction in the numerical analysis. [DOI: 10.1143/JJAP.47.6757]

KEYWORDS: GaN, micro array light-emitting diode, near-ultraviolet light-emitting diode, light extraction efficiency

1. Introduction

The III–nitride-based compounds such as AlGaN and InGaN have been successfully used to develop light-emitting diodes (LEDs) from ultraviolet (UV) to blue and green spectral regions.[1,2] For example, III–nitride-based blue and green LEDs have already been extensively used in full-color displays and highly efficient light source for traffic light lamps. UV emitters are of interest for fluorescence-based chemical sensing, flame detection, and possibly optical storage. Moreover, the invention of III–nitride-based LEDs is one of the key technological breakthroughs for solid-state lighting. However, the high refractive index of GaN prohibits light beyond a critical angle from being extracted owing to the total internal reflection. A large fraction of the generated light is trapped inside LED and absorbed by the nonradiation absorption centers. The internal absorption loss of LED increases as its chip size is increased, and finally, much more heat is generated. Several approaches and structures have been proposed and demonstrated to improve the output efficiency of III–nitride-based LEDs, such as surface texturing,[3–5] photonic crystals (PhCs),[6,7] micrometer-scale LEDs (μ-LEDs),[8,9] proper substrate shaping,[10] thin GaN structures,[11] and flip-chip packaging.[11]

The mechanism common to the first three approaches is to deteriorate the total internal reflection effect and consequently induce more photons emitting from LEDs. Surface texturing is one of the low-cost approaches. However, the random textured structure on the LED surface cannot be used to control the photonic behavior in a predictable manner. The two-dimensional PhCs with premeditated sub-wavelength structures on the LED surface can be regarded as a well-manipulated surface texturing with specified spatial frequencies to couple the light wave. Generally, PhCs are strongly dependent on the wavelengths, incident angles, and polarization states of incident waves. The LEDs are light sources with broadband spectra, nonplanar wavefronts, and random polarizations. These characteristics would result in the limited light extraction from LEDs with the surface integration of PhCs. The subwavelength PhC structure with a large surface-to-volume ratio is fabricated down to the p-GaN layer or even to quantum wells by dry etching. The thin transparent p-electrode cannot be evaporated only on the top facet of the PhC structure but evaporated on all edges surrounding the PhC structure. The p-metal on the damaged side-facets of the PhC structure would induce severe carrier loss owing to surface recombination. LEDs with an array of microstructures are expected to enhance the light extraction without degrading the electrical properties. Thus far, however, no evaluation has been made concerning the light extraction in LEDs with an array of microstructures. In general, it is considered that the enhanced light extraction of LEDs with an array of microstructures is attributable to the scattering of light from the etched sidewall surfaces and the marked increase in the surface areas. However, there is a lack of clarity on the extraction of the microstructures, such as which fraction of the emitted light can be extracted.

2. Analysis Method

In this study, the numerical and experimental demonstrations for the enhancement of light extraction efficiency in III–nitride-based LEDs with an array of microstructures are proposed. As shown in Fig. 1, a schematic diagram of the III–nitride-based LEDs with the deep etching of microstructures through the InGaN/GaN MQW active structure and down to the n-type GaN layer are fabricated on a sapphire (Al_2O_3) substrate. As illustrated in this figure, the structure parameters given in the following analysis include the period of microhole $\Lambda = 10\,\mu m$, microhole filling factor $f = 0.5$, indium–tin-oxide (ITO) thickness $h_{ITO} = 0.25\,\mu m$, p-type GaN layer thickness $h_{pGaN} = 0.3\,\mu m$, MQW thickness $h_{MQW} = 0.01\,\mu m$, n-type GaN layer thickness $h_{nGaN} = 0.49\,\mu m$, ITO refractive index $n_{ITO} = 1.8$, p-type GaN reflective index $n_{pGaN} = 2.5$, MQW reflective index $n_{MQW} = 2.4$, n-type GaN reflective index $n_{nGaN} = 2.5$, and microstructure etching depth $h_{mhole} = 1.05\,\mu m$. Multiple point sources with transverse electric (TE) and transverse magnetic (TM) polarizations in the MQW region are utilized in the finite-difference time domain (FDTD) analysis to model the behaviour of LEDs. As shown in Fig. 1, point sources are uniformly arranged in the MQW structure of every microstructure with a space resolution of 40 nm. It indicates that the interval between two point sources is

*E-mail address: mlwu@dop.ncu.edu.tw

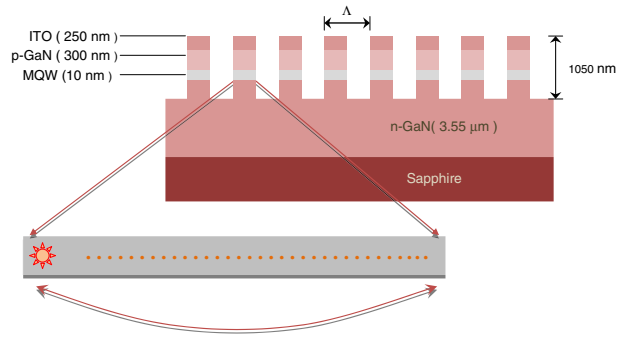

Fig. 1. (Color online) Schematic diagram of III–nitride-based LEDs with the deep etching of microstructures down to the n-type GaN layer.

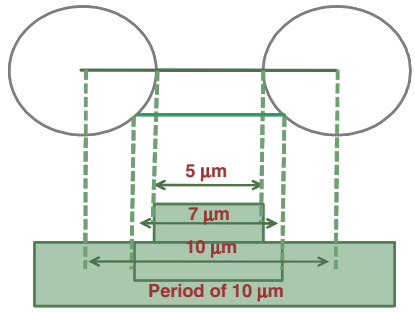

Fig. 2. (Color online) Schematic diagram with numerical analyses of microstructures considered in the same period with different filling factors.

approximately 300 nm because the microstructures can be regarded as a μLED with hole array. The numerical analyses of microstructures are considered in the same period with different filling factors as shown in Fig. 2. Such division of every different filling factor is 0.5 μm within one period. As a result of the incoherence of LED light sources, the linear summation of LED intensity distribution field with each filling factor is adopted. Moreover owing to the deep etching down to the n-type GaN layer, every microstucture on the proposed III–nitride-based LED can be regarded as a μLED. The behaviour of light emitting from one μLED and its effect on neighbouring microstrucutres would play an important role in the light extraction. Figure 3 shows a diagram of the simulated energy flux emitting from a single μLED on the proposed structure. As illustrated in this figure, the optical power emitting into the n-type GaN layer is much larger than that which escapes into the air. This deep-etching microstructure makes the light that penetrates into the n-type GaN layer scatter in various degrees as an optical aperture with a special numerical aperture (NA) that depends on the etching depth and width of this structure. Then, the power penetrating into the n-type GaN layer is converted to a guided mode and laterally extends in the layer up to a distance of ±25 μm. The neighbouring dummy microstructures would couple a partial power of the guided mode into the air. Since the period of the microstructures is up to 10 μm, the momentum of escaping light from the dummy microstructures is almost the same as that of the guided mode. It indicates that the escaping light that propagates in the air is the one with higher spatial frequencies.

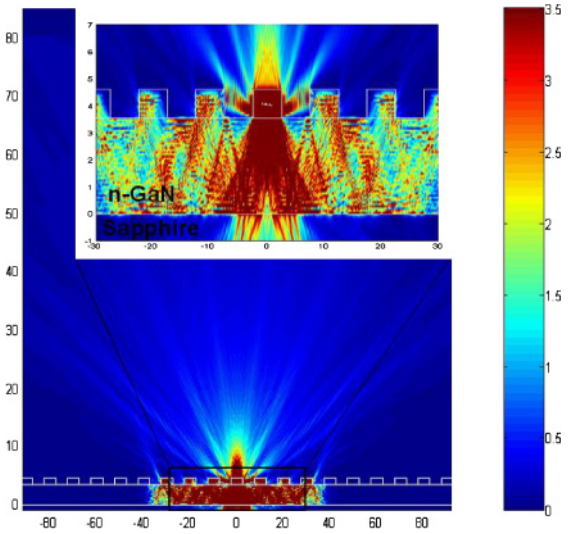

Fig. 3. (Color online) Diagram of simulated energy flux emitting from a single μLED on the proposed structure.

3. Experiments and Measurement

The near UV (n-UV) InGaN/GaN MQW LEDs used in this study were all grown on *c*-face (0001) 2-in. sapphire (Al_2O_3) substrates using a metal organic chemical vapor deposition (MOCVD) system. The epitaxial structure consists of a 30-nm-thick GaN nucleation layer, a 4-μm-thick Si-doped GaN n-cladding layer, an InGaN/GaN MQW active region, a 50-nm-thick Mg-doped $Al_{0.15}Ga_{0.85}N$ p-cladding layer, and a 0.25-μm-thick Mg-doped GaN layer. The MQW active region consists of seven periods of 3-nm-thick $In_{0.05}Ga_{0.95}N$ well layers and 15-nm-thick GaN barrier layers. After the growth, the surfaces of the samples are partially etched until the n-type GaN layers are exposed. Then, a 250-nm-thick ITO film is deposited onto the LED surfaces by e-beam evaporation to serve as the p-contacts. Standard photolithography and dry etching are subsequently used to form the microstructure pattern of the epitaxial structure. The etching depth of the epitaxial layers is controlled at 800 nm, which is more than the total p-layer thickness and MQW-layer thickness. In other words, the etching is stopped at the n-GaN region. For these types of LED, the strip width of the residual microstructure is 5 μm, while the spacing between the two lines is kept at 5 μm. The aperture rate (R_a) of the p-electrode outside the bond pad area is 67%. After the etching, Cr/Pt/Au are deposited onto the exposed n-type GaN layers to serve as the n-type electrodes. Figure 4 shows a top-view photograph of the meshed LED and an enlarged photograph of area A in the inset. It should be noted that the exposed n-GaN surface reveals the textured surface. It would be helpful for the improved light extraction efficiency from the exposed n-GaN surface. To study the mechanism of light extraction, the shallow etching of microstructures on the ITO p-contact is also carried out.

Figure 5 shows the measured light output power versus (*L–I*) curves of both LEDs with different microstructures, including the shallow etching of microstructures on the ITO p-contact (shallow etching on ITO) and the deep etching of microholes down to the n-type GaN layer (deep etching down to n-GaN). It is found that the output powers of these

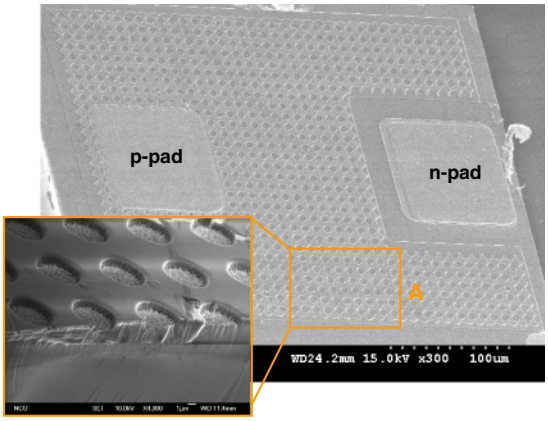

Fig. 4. (Color online) Top-view photograph of the LED with the deep etching of microstructures down to the n-type GaN layer and enlarged photograph of area A in the inset.

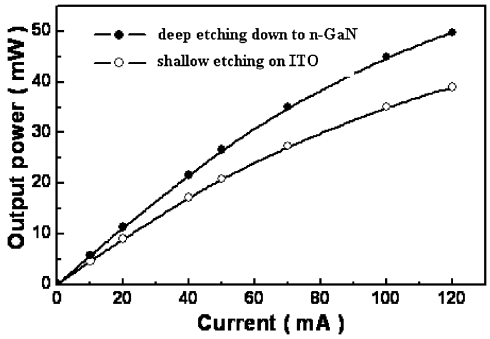

Fig. 5. Measured *L–I* curves of both LEDs with different microstructures, including the shallow etching of microstructures on the ITO p-contact (shallow etching on ITO) and the deep etching of microstructures down to the n-type GaN layer (deep etching down to n-GaN).

two LEDs both increased linearly with the increase of injection current. It is also found that the output power of the LED with deep-etching microstructure is larger than that with shallow etching on ITO. Under an injection current of 20 mA, the output powers are 9.0 and 11.3 mW for the microstructure ITO LED and the LED with deep-etching microstructure, respectively. Although the active region of the LED is reduced by 33% compared with that of the microstructure ITO LED, an enhancement in the extraction efficiency of 25.5% is obtained.

Figure 6 shows measured and simulated angular radiation patterns of the LED with deep-etching microstructures down to the n-type GaN layer (deep etching down to n-GaN) and the LED with shallow-etching microstructures on ITO (shallow etching on ITO). Both output beam patterns are measured at a dc driving current of 20 mA. Compared with the LED with a shallow etching on ITO, it can be seen clearly that the output beam pattern of the LED with a deep etching down to n-GaN is broader. It indicates that a large amount of light with high-frequency components is emitted from the LED with deep-etching microstructures. This phenomenon is the same as that predicted in the simulation. In the FDTD calculation, an enhancement in the extraction efficiency of 14% is obtained. As a result of the memory limitation of the computer used, the simulation was considered only in the three-dimensional (3-D)-like FDTD. The guided mode in the n-type GaN layer can be further

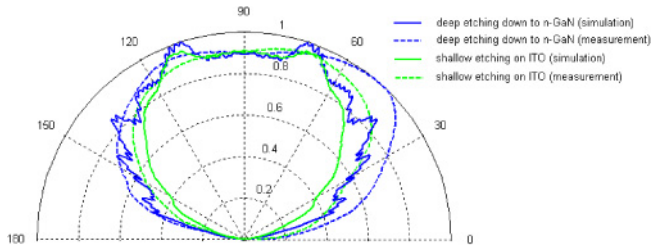

Fig. 6. (Color online) Measured and simulated angular radiation patterns of LED with deep-etching microstructure (deep etching down to n-GaN) and the ITO microstructure LED (shallow etching on ITO).

extended to another dimension; a deviation between the experimental and simulated extraction efficiencies of the LED with deep-etching microstructure occurs. The omnidirectional power penetrating into the n-type GaN layer is converted into several guided modes and extends in the layer laterally. Power confined in the guided modes can be effectively coupled into the air by the array of deep-etching microstructures. However, only a small amount of power in the GaN epilayers beneath the shallow-etching ITO microstructures can be converted into the guided modes of higher orders. The ITO microstructure cannot effectively couple the guided mode of the LED into the air. The angular radiation pattern of the LED with a shallow etching on ITO is almost a Lambertian pattern in the simulation and measurement.

4. Conclusions

In this paper, multiple point sources with TE and TM polarizations in the MQW region are utilized in the FDTD analysis to demonstrate the mechanism of enhanced light extraction efficiency in III–nitride-based LED with deep-etching microstructure. The simulation successfully explains the broad beam pattern observed in LEDs with deep-etching microstructures. It is verified that a large amount of light with high-frequency components can be coupled from the guided light by the deep-etching microstructures is the mechanism of enhancement in light output of III–nitride-based micro-array LEDs.

1) T. Mukai, M. Yamada, and S. Nakamura: Jpn. J. Appl. Phys. **38** (1999) 3976.
2) T. Mukai, M. Yamada, and S. Nakamura: Jpn. J. Appl. Phys. **37** (1998) 1358.
3) T. Fujii, Y. Gao, R. Sharma, E. L. Hu, S. P. DenBaars, and S. Nakamura: Appl. Phys. Lett. **84** (2004) 855.
4) S. I. Na, G. Y. Ha, D. S. Han, S. S. Kim, J. Y. Kim, J. H. Lim, D. J. Kim, K. I. Min, and S. J. Park: IEEE Photonics Technol. Lett. **18** (2006) 1512.
5) C. H. Kuo, C. C. Lin, S. J. Chang, Y. P. Hsu, J. M. Tsai, W. C. Lai, and P. T. Wang: IEEE Trans. Electron Devices **52** (2005) 2346.
6) A. David, T. Fuji, R. Sharma, K. McGroddy, S. Nakamura, S. P. DenBaars, E. L. Hu, and C. Weisbuch: Appl. Phys. Lett. **88** (2006) 061124.
7) C. H. Chao, S. L. Chung, and T. L. Wu: Appl. Phys. Lett. **89** (2006) 091116.
8) A. David, T. Fuji, B. Moran, S. Nakamura, S. P. DenBaars, R. Sharma, K. McGroddy, E. L. Hu, and C. Weisbuch: Appl. Phys. Lett. **88** (2006) 061124.
9) H. W. Choi, C. W. Jeon, and M. D. Dawson: IEEE Photonics Technol. Lett. **16** (2004) 33.
10) K. H. Kim, J. Li, S. X. Jin, J. Y. Lin, and H. X. Jiang: Appl. Phys. Lett. **83** (2003) 566.
11) M. Yamada, T. Mitani, Y. Narukawa, S. Shioji, I. Niki, S. Sonobe, K. Deguchi, M. Sano, and T. Mukai: Jpn. J. Appl. Phys. **41** (2002) 1431.